

1 Vertical Spatial Sensitivity and Exploration Depth of Low-Induction-Number
2 Electromagnetic-Induction Instruments

3 James B. Callegary^{a,*}, Ty P.A. Ferré^b and R.W. Groom^c

4

5 ^aU.S. Geological Survey, 520 N. Park Ave., Tucson, AZ 85719, USA

6 ^bHydrology and Water Resources, The Univ. of Arizona, Tucson, AZ 85721, USA

7 ^cR.W. Groom, PetRos EiKon Inc., 222 Snidercroft Rd., Concord, ON L4K 2K1, Canada

8 *Corresponding Author (jcallega@usgs.gov)

9

10

11 Any use of trade, product, or firm names in this publication is for descriptive purposes
12 only and does not imply endorsement by the U.S. Government.

13

14 ABSTRACT

15 Vertical spatial sensitivity and effective depth of exploration (d_e) of low-
16 induction-number (LIN) frequency-domain electromagnetic-induction instruments over a
17 layered soil were evaluated using a complete numerical solution to Maxwell's equations.
18 Previous studies using approximate mathematical solutions predicted a vertical spatial
19 sensitivity for instruments operating under LIN conditions that, for a given transmitter-
20 receiver coil-separation (s), coil orientation and transmitter frequency (ω), should depend
21 solely on depth below the land surface. When not operating under LIN conditions,
22 vertical spatial sensitivity and d_e also depend on apparent soil electrical conductivity (σ_a)
23 and therefore the induction number (β) which is directly proportional to σ_a . In this new

1 evaluation, we determine the range of σ_a and β values for which the LIN conditions hold
2 and how d_e changes when they do not. Two-layer soil models were simulated with both
3 horizontal (HCP) and vertical (VCP) coplanar coil orientations, $\omega = 9,800$ Hz and $s =$
4 3.66 m. Soil layers were given electrical conductivity values ranging from 0.1 to 200 mS
5 m^{-1} . As expected, d_e decreased as σ_a increased. Only the least electrically conductive soil
6 produced a d_e similar to that expected when operating under LIN conditions. For the VCP
7 orientation, this was 1.6 s, decreasing to 0.8 s in the most electrically conductive soil. For
8 the HCP orientation, d_e decreased from 0.76 s to 0.51 s. Differences between this and
9 previous studies are attributed to inadequate representation by the approximate solution
10 of: (1) skin-depth effect (attenuation and phase rotation of the fields traveling through the
11 medium) and (2) scattering at interfaces between layers. It is thus important to consider
12 the dependence of d_e on σ_a when using LIN FEM instruments to identify depth to targets
13 such as water tables, interfaces between soil or lithologic layers and variations in salt or
14 moisture content.

15

16 **Abbreviations:** σ , electrical conductivity; σ_a , apparent soil electrical conductivity; CS,
17 cumulative sensitivity; d_e , effective depth of exploration; FEM, frequency-domain
18 electromagnetic-induction; HCP, horizontal coplanar; LIN, low-induction-number; LS,
19 local sensitivity; VCP, vertical coplanar

20

INTRODUCTION

21 Low-induction-number frequency-domain electromagnetic-induction (LIN FEM)
22 instruments use the propagation of alternating electromagnetic fields through the soil to
23 measure the apparent soil electrical conductivity (σ_a) [mS m^{-1}]. This measured property is

1 a complicated average of spatially distributed localized electrical conductivities in the
2 subsurface. Apparent soil electrical conductivity is affected by several factors including
3 water content, mineralogy, temperature, soil texture, porosity, permeability, and salinity.
4 Instruments capable of operating as LIN FEM instruments include the EM38, EM31, and
5 EM34 (Geonics Limited, Mississauga, ON, Canada), the DUALEM instruments series
6 (DUALEM, Inc, Milton, ON) and the GEM instrument series (Geophex, Ltd., NC). The
7 range of applications of LIN FEM instruments for environmental and hydrologic
8 characterization and monitoring is large and ever increasing. Applications include aquifer
9 extent and water content studies (António and Pacheco, 2002; Schneider and Kruse,
10 2003; Sheets and Hendrickx, 1995), and lithology, soil salinity, and soil texture mapping
11 (Benjoudi et al., 2002; Lesch et al., 1998; Paine 2003; Stroh et al., 2001; Sudduth et al.,
12 2005; Triantafilis et al., 2005; Yoder et al., 2001). LIN FEM instruments also have been
13 used to delineate landfills (Lanz et al., 1998; Nyquist and Blair, 1991), contaminant
14 plumes (Matias et al., 1994), and areas of active recharge (Salama et al., 1994).

15 Quantitative applications of LIN FEM instruments to hydrologic investigations
16 depend on the ability to transform measured electrical conductivities into vertical and
17 horizontal variations of hydrologically relevant properties. The accuracy of these
18 transformations relies, primarily on (1) calibrating electrical conductivity to a property of
19 interest (e.g. volumetric water content) either through qualitative or numerical inversion,
20 and (2) mapping interpreted hydrologic variables based on measurement locations. A
21 comprehensive review of modeling and inversion as applied to electric and
22 electromagnetic methods was recently published by Pellerin and Wannamaker (2005). In
23 the present investigation, we exclusively examine the latter, less commonly considered

1 issue. Specifically, we use forward numerical models of layered soils to study the effect
2 of variations in σ_a on the vertical spatial sensitivity of LIN FEM instruments. This
3 information is useful when attempting to assign depths to properties such as soil water
4 content (e.g. depth to the water table), soil texture, salinity, and hydraulic conductivity.

5 It is commonly assumed that, under most conditions, the sample depth (or sample
6 volume in three-dimensions) of LIN FEM instruments is independent of the subsurface
7 electrical conductivity. McNeill (1980) defined “effective depths of exploration” (d_e)
8 based on the vertical spatial sensitivity of LIN FEM instruments in homogeneous and
9 horizontally layered soils, which he computed using an asymptotic approximation of
10 Maxwell’s equations. The asymptotic approximation is based on the assumption that the
11 induction number (β) is very small. (As such, this solution is sometimes referred to as the
12 “LIN approximation”, and it formed the basis for development of many LIN FEM
13 instruments.) The induction number is the ratio of the intercoil separation (s) (Fig. 1) to
14 the skin depth (δ) (Kaufman and Keller, 1983; Spies, 1989):

15

$$\beta = \frac{s}{\delta} = \frac{s}{\sqrt{\frac{2}{\sigma_a \omega \mu}}} \quad [1]$$

16 Where ω is angular frequency [s^{-1}], and μ is magnetic permeability [$Tm A^{-1}$] and μ
17 normally is assumed to be constant and equivalent to its free-space value (μ_0). Skin depth
18 is the depth at which the transmitted magnetic field strength has decayed to e^{-1} of its
19 initial magnitude at a reference point. In the low frequency limit, δ varies inversely with
20 the square root of σ_a . As σ_a increases, δ decreases and β increases, effectively decreasing
21 instrument sensitivity with increasing depth, and decreasing d_e . Some authors used the
22 LIN approximation in their investigations, but did not state the range of β required for a

1 valid approximation. McNeill (1980) asserted that the LIN approximation holds where β
2 is much less than 1 and recommended that LIN FEM instruments be used in
3 environments where $\sigma_a \leq 100 \text{ mS m}^{-1}$ (which for $\omega = 9,800 \text{ Hz}$ and $s = 3.66 \text{ m}$
4 corresponds to $\beta \leq 0.23$). Wait (1962) defined this as β less than about 0.3 and
5 Frischknecht (1987) defined the criterion as β less than 0.02. This disagreement makes it
6 unclear under what values of β the LIN approximation can be applied.

7 In this study, we use a standard commercial forward numerical code of
8 electromagnetic field propagation (EMIGMA, PetRos EiKon, Inc. 2004) to examine the
9 d_e of FEM instruments. A numerical code does not require the LIN approximation, and is
10 therefore more accurate in its representation of physical processes affecting
11 electromagnetic wave propagation and d_e of FEM instruments. A numerical code also
12 allows for identifying conditions under which the LIN approximation might not be
13 applicable. Specifically, like McNeill (1980), we define the vertical spatial sensitivity of
14 an FEM instrument in horizontally layered soil. Additionally, we vary σ_a to determine at
15 what β values the LIN approximation holds and when it does not, to determine the effect
16 on d_e . Based on our findings, we re-define the conditions under which the LIN
17 approximation should be used.

18

19

THEORY

20 LIN FEM instruments operate use with a transmitter coil to generate an
21 alternating magnetic field ($\partial \mathbf{H} / \partial t$) where \mathbf{H} is the magnetic field strength [A m^{-1}], t is
22 time [s], and bold H is a vector. This magnetic field propagates into the subsurface where
23 it induces alternating currents as described by Faraday's law:

1
$$\nabla \times \mathbf{E} = -\mu \frac{\partial \mathbf{H}}{\partial t} \quad [2]$$

2 where \mathbf{E} is electric field strength [V m^{-1}]. This equation states that a time varying
3 magnetic field will produce an electric field whose curl is equal to the negative of the
4 time derivative of the magnetic field. The electric field induces currents in the soil,
5 which, in turn, produce their own magnetic fields whose polarity and magnitude oppose
6 the change in the incident field. The incident magnetic field often is called the primary
7 field and the field generated by the induced currents is called the secondary field. These
8 two fields combine to induce currents in the receiver coil in accordance with Faraday's
9 law. The transmitter and receiver coils, and associated magnetic dipoles, can be oriented
10 relative to each other and to the soil surface. Orientations considered in this study were
11 horizontal coplanar (both coils lie flat on the ground) and vertical coplanar (coils are
12 upright and coplanar) (Fig. 1).

13 Maxwell's equations generally describe the macroscopic behavior of
14 electromagnetic fields (Gomez-Treviño et al., 2002). Numerical as well as analytical and
15 approximate solutions to these equations can be used to investigate the propagation of
16 subsurface electromagnetic fields under specific conditions. Typically, analytical
17 solutions can be derived only for simple scenarios like uniform half-spaces (Ward and
18 Hohmann, 1988). Even with geometric simplifications, additional restrictive simplifying
19 assumptions are required to solve the equations analytically. Approximate solutions, such
20 as the solution used by McNeill (1980), use restrictive physical and mathematical
21 assumptions to arrive at solutions that are approximately valid in some limited physical
22 regime. Numerical codes developed in the 1980s (Anderson, 1984; Tabbagh, 1985;
23 Wannamaker et al., 1984) allow for consideration of more complex, realistic soil models.

1 In the development of EMIGMA, the code used for this study, an attempt was made not
2 to simplify the mathematics in any way. Although small numerical errors still result from
3 the calculations, errors in EMIGMA are generally less than errors expected from
4 instruments or geologic noise. In addition to allowing for more general geometries,
5 numerical codes can more accurately represent processes such as skin depth affects and
6 scattering. Scattering, which includes reflection, refraction, current channeling, and
7 induction, describes the distortion of electromagnetic waves at spatial discontinuities in
8 electrical and magnetic properties of soil. These various processes affect propagation of
9 the incident electromagnetic field and consequently the propagation and magnitude of
10 secondary electromagnetic fields.

11 McNeill's (1980) white paper discussed part of the theory and assumptions of the
12 mathematical approximations that provide the basis for development, use, and
13 interpretation of LIN FEM instruments. The derivation of equations discussed in
14 McNeill's paper was developed in greater detail by Belluigi (1949), Wait (1955, 1962),
15 Kaufman and Keller (1983), and Gomez-Treviño et al. (2002). The LIN approximation is
16 derived from Maxwell's equations for a one-dimensional soil (homogeneous, layered, or
17 arbitrary electrical conductivity (σ) variations with depth) in which transmitter frequency
18 is low and the distance (s) between a transmitting magnetic dipole and a receiver (Fig. 1)
19 is small compared to the skin depth (δ) [m] of magnetic fields in the soil (LIN
20 conditions). For these conditions, vertical spatial sensitivity and d_e are independent of σ_a
21 and the LIN approximation is valid. However, opinions on what constitutes LIN
22 conditions can vary by investigator. For an EM31 instrument with a coil spacing of 3.66
23 m and an operating frequency of 9,800 Hz, the LIN assumptions might be valid for σ_a

1 <200 mS m⁻¹ for Wait's (1962) criterion, ≤100 mS m⁻¹ for McNeill's (1980), or < 0.8 mS
 2 m⁻¹ for Frischknecht's (1987). Table 1 shows the corresponding values for resistivity and
 3 skin depth. A practical difference exists between 0.8 mS m⁻¹ and the two higher values.
 4 Electrical conductivity of most surficial material in the continental United States likely
 5 lies between 0.8 and 100 mS m⁻¹ (Keller and Frischknecht, 1966). If either McNeill's or
 6 Wait's criterion is correct, then the LIN approximation and McNeill's associated guides
 7 to data interpretation should be able to be used without significant problems. If
 8 Frischknecht's is the correct criterion, however, soil and rock electrical conductivities at
 9 most field sites likely are too high for the LIN approximation to be valid. As a result,
 10 inferences of true σ_a , and thicknesses and numbers of soil layers based on these
 11 assumptions could be incorrect.

12 When site characteristics and instrument parameters combine to satisfy the LIN
 13 conditions, the quadrature component of the secondary magnetic field strength, H_s , is
 14 linearly dependent on σ_a (McNeill, 1980). The quadrature component of the secondary
 15 magnetic field is that part of the secondary magnetic field that is 90° out of phase with the
 16 primary field (Telford et al., 1990):

$$17 \quad \sigma_a = \frac{4}{\omega \mu_o s^2} \frac{(H_s)_{\text{Quadrature Component}}}{H_p} \quad [3]$$

18 Where H_p is the primary magnetic field strength. For a given measurement of σ_a , coil
 19 orientation, s and ω usually are fixed; however if s is increased or ω decreased, d_e
 20 increases. The effective depth of exploration will also increase by changing the magnetic
 21 dipole orientation from horizontal (HCP) to vertical (VCP), because VCP sensitivity
 22 distribution peaks at greater depths than the HCP distribution (Fig. 2).

1 McNeill (1980) provided a simple form of spatial sensitivity analysis using his
 2 “cumulative response”, which we change to “cumulative sensitivity”, (a measure of an
 3 instrument’s distribution of sensitivity in the subsurface). Cumulative sensitivity (CS) can
 4 be used to determine sensitivity of LIN FEM instruments to all material above or below a
 5 given depth. Depths are normalized to facilitate comparisons of instruments with
 6 different intercoil separations. The normalized depth, z , is the actual depth divided by the
 7 intercoil separation, s , and is referred to in terms of s . For instance, a 7.32 m depth for an
 8 instrument with a 3.66-m intercoil separation is referred to as $2 s$. Equations of
 9 cumulative sensitivity for the horizontal (CS_{HCP}) and vertical (CS_{VCP}) coil orientations as
 10 a function of normalized depth (McNeill, 1980) are:

$$11 \quad CS_{HCP}(z) = \int_z^{\infty} LS_{HCP}(z) dz = \frac{1}{(4z^2 + 1)^{1/2}} \quad [4]$$

$$12 \quad CS_{VCP}(z) = \int_z^{\infty} LS_{VCP}(z) dz = (4z^2 + 1)^{1/2} - 2z \quad [5]$$

13 where local sensitivity (LS) is the relative contribution of material at a given depth to the
 14 measured value of σ_a . A CS value represents the fraction of the secondary field at the
 15 receiver that originates between a depth z and infinite depth. When z is small and CS is
 16 near 1, most of the measured response comes from soil at a depth greater than z . The part
 17 of the response due to material in the interval between the surface ($z = 0$) and z is $1-CS$.
 18 By plotting the functions in Eqs. [4] and [5], and locating the CS value associated with
 19 McNeill’s exploration depths, it appears that McNeill used a CS value of 0.7 (or 70
 20 percent) to define d_e (McNeill, 1980, p. 5-6). For example, when $CS = 0.3$ for HCP
 21 orientation, about 30 percent of the measured response is attributable to material at depths
 22 greater than $0.76 s$ (Fig. 2). Therefore, the interval between $0 s$ and $0.76 s$ contributes 70

1 percent of the HCP orientation response. Material located between 0 and 1.6 s contributes
2 70 percent of the VCP orientation response (Fig. 2). These depths, 0.76 s and 1.6 s ,
3 represent d_e for these orientations under LIN conditions.

4 In a two-layer soil, for which CS is calculated from infinite depth to the contact
5 between the layers, the top layer's contribution to the measured response is $1-CS$. In such
6 soil, CS near 1 represents a nearly homogeneous soil where σ_a is equal to σ of the lower
7 layer. Cumulative sensitivity near 0 represents a nearly homogeneous soil where σ_a is
8 equal to σ of the upper layer. In a two-layer soil, σ_a can be calculated by:

$$9 \quad \sigma_a = \sigma_{Layer1}(1 - CS) + \sigma_{Layer2}CS \quad [6]$$

10 This calculation is equivalent to equation 5 from McNeill (1980). The cumulative
11 sensitivity can be determined based on σ_a of a two-layered soil if σ values of each layer
12 (σ_{Layer1} , σ_{Layer2}) are known. Specifically, rearranging Eq. [6] to solve for CS gives:

$$13 \quad CS = \frac{\sigma_a - \sigma_{Layer1}}{\sigma_{Layer2} - \sigma_{Layer1}} \quad [7]$$

14

15

METHODS

16 In this study, the software EMIGMA (PetRos EiKon Inc., 2004) was used to
17 conduct forward numerical simulations of a Geonics EM31 instrument response over a
18 nearly homogeneous or horizontally layered soil. The software was developed to
19 calculate three-dimensional, electromagnetic-field propagation in complex environments
20 for a great variety of instrument systems. The code, prior to commercial release, was
21 calibrated against a number of academic and internal industry codes, as well as codes
22 published in several articles and doctoral theses. An intercoil separation of 3.66 m and a

1 transmitting frequency of 9,800 Hz were used for all simulations. These are the
2 instrument parameters of used in Geonics EM31 instrument. The software represents
3 coils as alternating magnetic dipoles which for these simulations were placed 0.05 m
4 above ground. Magnetic permeability was constant for all simulations and set equal to its
5 free-space value (μ_0). The ratio of the secondary to the primary magnetic field magnitude,
6 in percent, was used as output format instead of σ_a , because this is the more common
7 output format of many instruments. Moreover, σ_a is inherently less accurate than the
8 magnetic field ratio because it can only be calculated through the use of numerical
9 inversion routines or approximate models.

10 All results are presented as *CS* for direct comparison with results of LIN
11 approximation. We simulated two-layer soils differing only in σ of the layers. Individual-
12 layer electrical conductivities ranged from 0.1 to 200 mS m⁻¹. In each two-layered soil,
13 upper and lower layer σ varied from nearly equal (e.g. upper layer 99 mS m⁻¹, lower layer
14 100 mS m⁻¹), to very different values (e.g. upper layer 100 mS m⁻¹, lower layer 0.1 mS m⁻¹).
15 For each σ -value used in the simulations, the response (ratio of magnetic field
16 magnitudes) was determined for a homogeneous half-space for both horizontal- and
17 vertical-coplanar coil orientations. A series of simulations was then carried out by
18 varying upper layer thickness. Equation 7 was used to determine the numerical *CS* value
19 from the simulation results. One value in the *CS* distribution was calculated from each
20 simulation. Each *CS* value was plotted as a function of depth to the interface between
21 layers to generate a curve for comparison with curves in figure 2. Comparing LIN-
22 approximation curves facilitated determining the effects of changing individual-layer
23 electrical conductivities on the vertical spatial sensitivity distribution.

1 Cumulative sensitivity was calculated for two soil-model types: Type 1 and Type
2 2 (Fig. 3). For a given series of simulations, a constant- σ upper layer was used for Type 1
3 soil models and constant- σ lower layer was used for Type 2 soil models. Each model type
4 was evaluated at two ranges of σ_a , one electrically “resistive” and one electrically
5 “conductive”, in which the soil model was composed of two layers and thickness of the
6 top layer ranged from 0.001 to 18 m (or 0 to 4.9 s). For all soil models, the bottom layer
7 was essentially infinitely thick (1×10^8 m). For Type 1 resistive soil models, σ of the
8 upper layer was held constant at 0.1 mS m⁻¹ and σ of the lower layer was given one of
9 three values: 0.2, 10, or 100 mS m⁻¹. For Type 2 resistive soil models, σ of the upper
10 layer was given values of 0.2, 10, or 100 mS m⁻¹, and σ of the lower layer was held
11 constant at 0.1 mS m⁻¹. These resistive soil models were used to match the LIN
12 approximate solution and to study vertical sensitivity distribution changes in more
13 electrically resistive environments. To mimic conditions common in near-surface
14 investigations, a series of electrically conductive simulations were carried out at higher σ_a
15 values using the same Type 1 and 2 soil-model scenarios. Such conditions might be
16 found at waste sites contaminated with inorganic compounds, at landfills or in saturated
17 clays. The constant- σ layer was 100 mS m⁻¹ and five soils were simulated in which the
18 variable layer σ ranged from 0.1 to 200 mS m⁻¹.

19

20

RESULTS AND DISCUSSION

21

22

23

Cumulative sensitivity was plotted as a function of depth to the interface between upper and lower layers to compare the vertical sensitivity distribution of the LIN approximation over a layered soil with those derived from numerical simulations (Figs.

1 4-6). Except for two soils with a 200 mS m⁻¹ layer, σ in all simulated soils was less than
2 or equal to 100 mS m⁻¹ (one of McNeill's (1980) criteria for the LIN conditions). A soil
3 model in which upper layer σ was 0.1 mS m⁻¹ and lower layer σ was 0.2 mS m⁻¹ is
4 referred to as the [0.1/0.2] soil model. Induction numbers calculated from the results of
5 simulations ranged from a minimum of about 0.01 for the [0.1/0.2] and [0.2/0.1] soil
6 models to between 0.23 and 0.32 for the [100/200] and [200/100] soil models (Table 1).
7 One conclusion of the LIN approximation is that vertical sensitivity, and therefore d_e ,
8 does not depend on σ_a . However, results of simulations indicate that instrument spatial
9 sensitivity varies significantly with changes in σ_a . This was true for Type 1 and 2 models
10 for both homogeneous, (e.g., the [0.1/0.2] and [100/99] soil models), as well as
11 heterogeneous soil models. The general shape of all cumulative sensitivity distributions
12 was similar to that predicted by the LIN approximation. In the more electrically resistive
13 soils simulated, [0.1/0.2] and [0.2/0.1], CS values were close to those predicted by the
14 LIN approximation (Fig. 4). In soils with higher σ_a , however, the simulated CS values
15 were at shallower depths than comparable LIN approximation values. For example, in
16 Fig. 4A, the HCP LIN approximation predicts a CS value of 0.2 will occur at a depth of
17 about 2.5 s . In contrast, the numerical approach predicts that as σ increases, the CS depth
18 decreases from just under 2.5 s for the [0.2/0.1] and [0.1/0.2] soil models to 2.0, 1.8, and
19 1.5 s for the [0.1/10], [10/0.1], and [0.1/100] soil models, respectively. The minimum CS
20 depth was about 1.2 s for the [100/0.1] soil model. Although nearly all simulated σ_a
21 values are within the LIN range indicated by McNeill (1980) and Frischknecht (1987),
22 only simulations of the [0.1/0.2] and [0.2/0.1] soil models ($\beta \approx 0.01$) came close to the
23 vertical sensitivity distribution predicted by the LIN approximation (Fig. 4). This

1 indicates that only for electrically resistive soils do the LIN approximation and its
2 predictions of the effective depth of exploration hold. Thus for many soils, depth to
3 targets such as the water table or a particular soil horizon may be misjudged even at
4 moderate values of σ_a . For electrically conductive soils, for instance those that are clay-
5 rich, salty or wet, such targets may be missed entirely.

6 There were a number of similarities and differences between the results of Type 1
7 and 2 soil-model simulations. In both model types, lower CS values occurred in soil with
8 the higher upper-layer σ . For instance, in the [0.1/10] and [10/0.1] soil models, lower CS
9 values were in the [10/0.1] soil model. This indicates that a LIN instrument would be less
10 sensitive at depth to a soil with a [10/0.1] layering than to one with a [0.1/10] layering.
11 Thus, it may be difficult to distinguish temporal or spatial variability of σ_a , for example
12 while tracking changes in salt or moisture content, below an electrically conductive
13 surface layer. For a given σ -contrast, soil models with varied lower-layer σ (Type 1) were
14 more similar to one another than soil models with varied upper-layer σ (Type 2). Deeper
15 layers seemed to have less effect on VCP results than on HCP results, probably because
16 the VCP orientation was more sensitive to shallow depths than HCP orientation. For both
17 orientations, Type 1 curves are more similar to one another than Type 2 curves, possibly
18 because the source of variability, the top layer, is closer to the instrument. The last
19 similarity to note is that, at any given depth, a non-linear decrease in CS values occurred
20 as the electrical conductivity of either layer increased. All these trends also occurred in
21 higher conductivity soil models (Figs. 5 and 6).

22 McNeill's (1980) criterion for identifying d_e was $CS = 0.3$. Using this criterion for
23 each numerical model, we determined d_e by locating the depth on each curve that

1 corresponded to a CS value of 0.3 (Figs. 4-6). In contrast to previous findings, d_e
2 decreased with increasing σ_a (Fig. 7). This deviation from the LIN approximation was
3 found in all soils simulated, including homogeneous and heterogeneous soils. The effect
4 of increasing electrical conductivity on d_e was different for each coil orientation. For the
5 VCP orientation, d_e for all numerical models tested ranged from 1.6 s, the same depth as
6 the LIN approximation, to about 0.8 s for the most electrically conductive soil. Using the
7 VCP LIN d_e could result in an overestimate of depth to soil-layer interfaces by as much
8 as 100 percent of the actual d_e . For the HCP orientation, d_e ranged from 0.76 s to 0.51 s.
9 Using the VCP LIN d_e could result in an overestimate of as much as 50 percent.
10 Deviations of 10 percent or more from the LIN predicted depths occurred at σ_a values of
11 3 mS m⁻¹ or greater. Given the range of near-surface σ_a in the continental USA (Keller
12 and Frischknecht, 1966), reliance on the LIN assumptions at many field sites could lead
13 to significant overestimates of d_e and poor estimates of layer thickness and composition,
14 water content or depth to interfaces such as the water table or changes in soil texture.

15 Considering the range of β , differences between the LIN and numerical
16 approaches likely are caused by skin affect and scattering phenomena, which are not
17 adequately represented by the LIN approximation. Scattering can affect both primary and
18 secondary magnetic fields. Both processes affect the cumulative secondary field sensed
19 by the instruments at the surface. As a result, vertical variations in electrical conductivity
20 will affect the results of field surveys by changing vertical spatial sensitivity. Temporal
21 variations in water content, soil temperature, and salinity cause temporal variations in σ_a ,
22 which may change d_e . At any field site where physical, chemical, or hydraulic properties
23 are spatially non-uniform, d_e is also likely to be non-uniform. Although the numerical

1 data plotted in figure 7 will allow for a better understanding of the behavior d_e with
2 change in σ_a , accurate determination of d_e may be difficult without the aid of numerical
3 simulations.

4

5 **CONCLUSIONS**

6 Vertical spatial sensitivity and the effective depth of exploration of low-induction-
7 number frequency-domain electromagnetic (LIN FEM) instruments in two-layer soils
8 were studied using an industry-standard numerical model. The model simulation results
9 were compared to interpretations based on the LIN asymptotic approximation developed
10 previously. Clear differences were indicated between the predictions of the approximate
11 and numerical approaches. In the numerical simulations, the effective depth of
12 exploration decreased by up to 50 percent as the electrical conductivity of the soil
13 increased when compared with the predictions of the LIN approximation. In the LIN
14 approximation, vertical spatial sensitivity and effective depth of exploration are
15 independent of the apparent soil electrical conductivity. In contrast, the numerical models
16 indicate that magnitude and distribution of soil properties affecting electrical conductivity
17 in the subsurface can significantly alter LIN instruments' vertical spatial sensitivity and
18 consequently their effective depth of exploration. In electrically resistive soil models,
19 where induction numbers were small (induction number ≤ 0.01 for a 0.1 mS m^{-1} upper
20 layer over 0.2 mS m^{-1} lower layer soil model), the vertical sensitivity distribution was
21 similar to that predicted using the LIN asymptotic approximation. Under more
22 electrically conductive conditions, even those that meet the low-induction-number criteria
23 of previous authors, a lower cumulative sensitivity than that predicted by the LIN

1 approximation was observed at a given depth. The results indicate that in hydrologic and
2 environmental investigations in any but the most electrically resistive environments, LIN
3 FEM instrument sensitivity will likely be focused closer to the surface than predicted by
4 the LIN approximation. This has important implications for studies of soil or geologic
5 layering, water table detection, studies of soil salinity, contaminant transport and landfill
6 delineation. In short, all studies that use LIN FEM instruments to study the vertical
7 distribution of properties in the subsurface need to incorporate this information into
8 project planning and data analysis. More heterogeneous subsurface conditions will
9 benefit from numerical simulation of electromagnetic wave propagation to aid in the
10 attribution of hydrologic properties, inferred from LIN FEM measurements, to
11 appropriate subsurface locations. However, when access to software, time or resources
12 does not allow for numerical modeling, our plot of effective depth of exploration versus
13 apparent soil electrical conductivity may be used to estimate the effective depth of
14 exploration based on reasonable estimates of the subsurface electrical conductivity.

REFERENCES

- 1
2 Anderson, W.L., 1984. Computation of Green's tensor integrals for three-dimensional
3 electromagnetic problems using fast Hankel transforms. *Geophysics* 49(10):1754-
4 1759.
- 5 António, F. and L. Pacheco. 2002. Response to pumping of wells in sloping fault zone
6 aquifers. *J. Hydrol.* 259:116-135.
- 7 Belluigi, A. 1949. Inductive coupling of a homogeneous ground with a vertical coil.
8 *Geophysics* 14(4):501-507.
- 9 Benjoudi, H., P. Weng, R. Guérin, and J.F. Pastre. 2002. Riparian wetlands of the middle
10 reach of the Seine river (France). historical development, investigation and present
11 hydrologic functioning: A case study. *J. Hydrol.* 263:131-155.
- 12 Frischknecht, F.C. 1987. Electromagnetic physical scale modeling. p. 365-441. *In* M.N.
13 Nabighian, , and J.D. Corbett (eds.) *Electromagnetic methods in applied geophysics.*
14 *Vol 1: Soc. Expl. Geophys.*
- 15 Gomez-Treviño, E., F.J. Esparza, and S. Méndez-Delgado. 2002. New theoretical and
16 practical aspects of electromagnetic soundings at low induction numbers. *Geophysics*
17 67(5):1441-1451.
- 18 Kaufman, A.A., and G.V. Keller. 1983. *Frequency and transient soundings.* Elsevier,
19 New York.
- 20 Keller, G.V., and F.C. Frischknecht. 1966. *Electrical Methods in Geophysical*
21 *Prospecting.* Pergamon Press, New York.

- 1 Lanz, E., D.E. Boerner, H. Maurer, and A. Green. 1998. Landfill delineation and
2 characterization using electrical, electromagnetic and magnetic methods. *J. Environ.*
3 *Eng. Geophys.* 3(4):185-196.
- 4 Lesch, S.M., J. Herrero, and J.D. Rhoades. 1998. Monitoring for temporal changes in soil
5 salinity using electromagnetic induction techniques. *Soil Sci. Soc. Am. J.* 62:232-242.
- 6 Matias, M.S., M. Marques da Silva, P. Ferreira, and E. Ramalho. 1994. A geophysical
7 and hydrogeological study of aquifers contamination by a landfill. *Appl. Geophys.*
8 32:155-162.
- 9 McNeill, J.D. 1980. Electromagnetic terrain conductivity measurement at low induction
10 numbers. Technical Note TN-6. Geonics Limited, Mississauga, Ontario, Canada.
- 11 Nyquist, J.E., and M.S. Blair. 1991. A geophysical tracking and data logging system.
12 Description and case history. *Geophysics* 56(7):1114-1121.
- 13 Paine, J.G., 2003. Determining salinization extent, identifying salinity sources, and
14 estimating chloride mass using surface, borehole, and airborne electromagnetic
15 induction methods. *Water Resour. Res.* 39(3):1059, doi.10.1029/2001WR000710.
- 16 Pellerin, L., and P.E. Wannamaker. 2005. Multi-dimensional electromagnetic modeling
17 and inversion with application to near-surface earth investigations. *Comput. Electron.*
18 *Agric.* 46:71-102.
- 19 PetRos EiKon, Inc. 2004. EMIGMA. Release 7.7. PetRos EiKon, Inc., Concord, ON,
20 Canada.
- 21 Salama, R.B., G. Bartle, P. Farrington, and V. Wilson. 1994. Basin geomorphological
22 controls on the mechanism of recharge and discharge and its effect on salt storage and
23 mobilization -- comparative study using geophysical surveys. *J. Hydrol.* 155:1-26.

- 1 Schneider, J.C., and S.E. Kruse. 2003. A comparison of controls on freshwater lens
2 morphology of small carbonate and siliciclastic islands. examples from barrier islands
3 in Florida, USA. *J. Hydrol.* 284:253-269.
- 4 Sheets, K.R., and J.M.H. Hendrickx. 1995. Noninvasive soil water content measurement
5 using electromagnetic induction. *Water Resour. Res.* 31(10):2401-2409.
- 6 Spies, B.R. 1989. Effective depth of exploration in electromagnetic sounding methods.
7 *Geophysics* 54(7):872-888.
- 8 Stroh, J.C., S. Archer, J.A. Doolittle, and L. Wilding. 2001. Detection of edaphic
9 discontinuities with ground-penetrating radar and electromagnetic induction.
10 *Landscape Ecol.* 16:377-390.
- 11 Sudduth, K.A., N.R. Kitchen, W.J. Wiebold, W.D. Batchelor, G.A. Bollero, D.G.
12 Bullock, D.E. Claye, H.L. Palm, F.J. Pierce, R.T. Schuler, K.D. Thelen. 2005.
13 Relating apparent electrical conductivity to soil properties across the north-central
14 plains. *Comput. Electron. Agric.* 46:263-283.
- 15 Tabbagh, A. 1985. The response of a three-dimensional magnetic and conductive body in
16 shallow depth electromagnetic prospecting. *Geophysical J. Roy. Astr. S.* 81:215-230.
- 17 Telford, W.M., L.P. Geldart, and R.E. Sheriff. 1990. *Applied geophysics.* Cambridge
18 University Press, Cambridge, MA.
- 19 Triantafilis, J., and S.M. Lesch. 2005. Mapping clay content variation using
20 electromagnetic induction techniques. *Comput. Electron. Agric.* 46:203-237.
- 21 Wait, J.R. 1955. Mutual electromagnetic coupling of loops over a homogeneous ground.
22 *Geophysics* 20(3):630-637.

1 Wait, J.R. 1962. A note on the electromagnetic response of a stratified earth. *Geophysics*
2 27(3):382-385.

3 Wannamaker, P.E., G.W. Hohmann, and W.A. SanFilipo. 1984. Electromagnetic
4 modeling of three-dimensional bodies in layered earths using integral equations.
5 *Geophysics* 49(1):60-74.

6 Ward, S.H. and G.W. Hohmann. 1988. Electromagnetic theory for geophysical
7 applications. p. 131-312. *In* M.N. Nabighian (ed.) *Electromagnetic methods in*
8 *applied geophysics, Vol 1: Soc. Expl. Geophys.*

9 Yoder, R.E., R.S. Freeland, J.T. Ammons, and L.L. Leonard. 2001. Mapping agricultural
10 fields with GPR and EMI to identify offsite movement of agrochemicals. *J. Appl.*
11 *Geophys.* 47:251-259.

12

1 Vertical Spatial Sensitivity and Exploration Depth of Low-Induction-Number
2 Electromagnetic-Induction Instruments

3 James B. Callegary^{a,*}, Ty P.A. Ferré^b and R.W. Groom^c

4 **FIGURE and TABLE CAPTIONS**

5

6 Table 1. Induction number calculated for electrical conductivities with low-induction-number
7 condition criteria proposed by several researchers.

8

9

10 Figure 1. LIN FEM instruments, two coils with an intercoil separation (s). One coil transmits
11 (Tx) the primary magnetic field and one coil receives (Rx) a combination of the primary and
12 secondary fields. Coils may be oriented either horizontally or vertically with respect to ground
13 surface as indicated by directional arrows.

14

15 Figure 2. Cumulative sensitivity and relative depth to interface between layers, McNeill (1980).
16 Approximations are for vertical (VCP) and horizontal (HCP) coplanar coil orientations.
17 McNeill's "effective depth of exploration" is indicated by a cumulative sensitivity value of 0.3.
18 Cumulative sensitivity of low-induction-number (LIN) instruments is calculated from infinity to a
19 given relative depth. Relative depth is depth divided by intercoil separation.

20

21 Figure 3. Each set of cumulative-sensitivity simulations was based on a two-layer soil. Electrical
22 conductivity of the upper layer in soil model Type 1 and the lower layer in soil model Type 2
23 were fixed at 0.1 mS m^{-1} for the electrically resistive case or 100 mS m^{-1} for the electrically
24 conductive case. The variable electrical-conductivity layer was given values ranging from 0.1 to

1 200 mS m⁻¹. For a given two-layer soil model in each set of simulations, the thickness of the
2 upper layer increased from 0.001m to 18 m. Tx indicates transmitter coil; Rx indicates receiver
3 coil; and s is intercoil separation.

4

5 Figure 4. Cumulative sensitivity for soil model Types 1 and 2 calculated from forward
6 numerical simulation results compared with low-induction-number (LIN) approximation.
7 (A) horizontal (HCP) and (B) vertical (VCP) coplanar coil orientation. Relative depth is
8 depth divided by intercoil separation. The first number in brackets is the upper layer
9 electrical conductivity, in mS m⁻¹; the second number is lower layer electrical
10 conductivity. In (B), to show underlying LIN VCP approximation curves, the lines for the
11 VCP [0.1/0.2] and [0.2/0.1] soil models were removed.

12

13 Figure 5. Soil model Type 1 cumulative sensitivity using the higher electrical conductivities
14 sometimes detected in environmental investigations. Comparison of results of forward numerical
15 simulation results with the low-induction-number (LIN) approximation. (A) is horizontal (HCP)
16 and (B) is vertical (VCP) coplanar coil orientation. Relative depth is depth divided by intercoil
17 separation. The first number in brackets is the upper layer electrical conductivity, in mS m⁻¹, the
18 second number is that of the lower layer.

19

20 Figure 6. Soil model Type 2 cumulative sensitivity using the higher electrical conductivities
21 sometimes detected in environmental investigations. Comparison of results of forward numerical
22 model simulation results with the low-induction-number (LIN) approximation. (A) is horizontal
23 (HCP) and (B) is vertical (VCP) coplanar coil orientation. Relative depth is the depth divided by
24 the intercoil separation. The first number in brackets is the upper layer electrical conductivity, in
25 mS m⁻¹, the second number is the lower layer electrical conductivity.

1

2 Figure 7. Relation between apparent electrical conductivity and effective depth of exploration:
3 comparison of simulated and LIN approximation results. VCP, vertical coplanar coil orientation;
4 HCP, horizontal coplanar coil orientation. Effective depth of exploration is the depth divided by
5 the intercoil separation.

1

Apparent soil electrical conductivity, σ_a (mS m ⁻¹)	Resistivity, σ^{-1} (ohm-m)	Skin depth, δ (m)	Induction number, β (--)	LIN condition criterion ($\beta \leq x$) proposed by:
10,000	0.1	2	2.3	n/a
1,000	1	5	.72	n/a
500	2	7	.51	n/a
200	5	11	.32	Wait (1962)
100	10	16	.23	McNeill (1980)
50	20	23	.16	n/a
20	50	36	.10	n/a
10	100	51	.072	n/a
5	200	72	.051	n/a
2	500	114	.032	n/a
0.8	1,300	183	.020	Frischknecht (1987)
0.2	5,000	359	.010	n/a
0.1	10,000	508	.007	n/a
0.01	100,000	1,608	.002	n/a
Frequency (Hz)	9,800			
Coil Spacing (m)	3.66			
Magnetic permeability of free space (H m ⁻¹)	$4\pi \times 10^{-7}$			

2

3

Table 1. Induction number calculated for electrical conductivities with low-induction-number condition criteria proposed by several researchers.

4

5

1

2

3

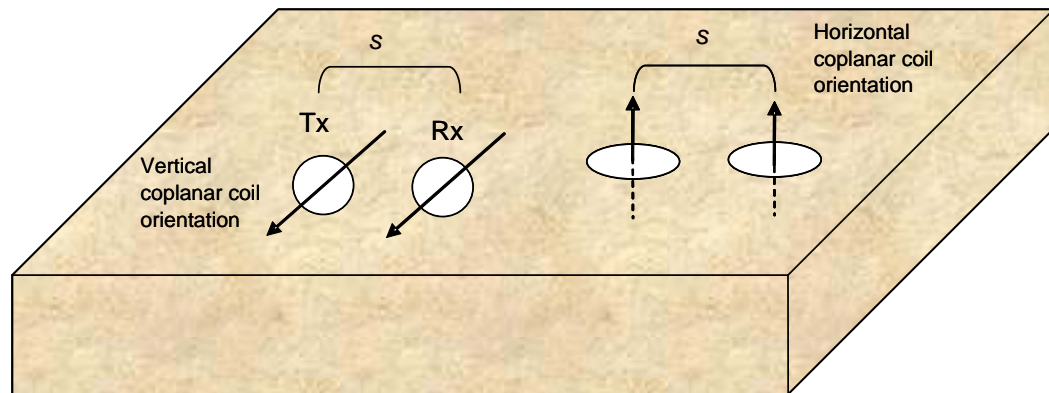
4

5

6

7

8



9

10

11

12

Figure 1. LIN FEM instruments, two coils with an intercoil separation (s). One coil transmits (Tx) the primary magnetic field and one coil receives (Rx) a combination of the primary and secondary fields. Coils may be oriented either horizontally or vertically with respect to ground surface as indicated by directional arrows.

1
2
3
4
5
6
7
8
9
10
11
12
13
14
15
16
17
18
19
20
21
22
23
24
25
26
27
28
29
30
31
32

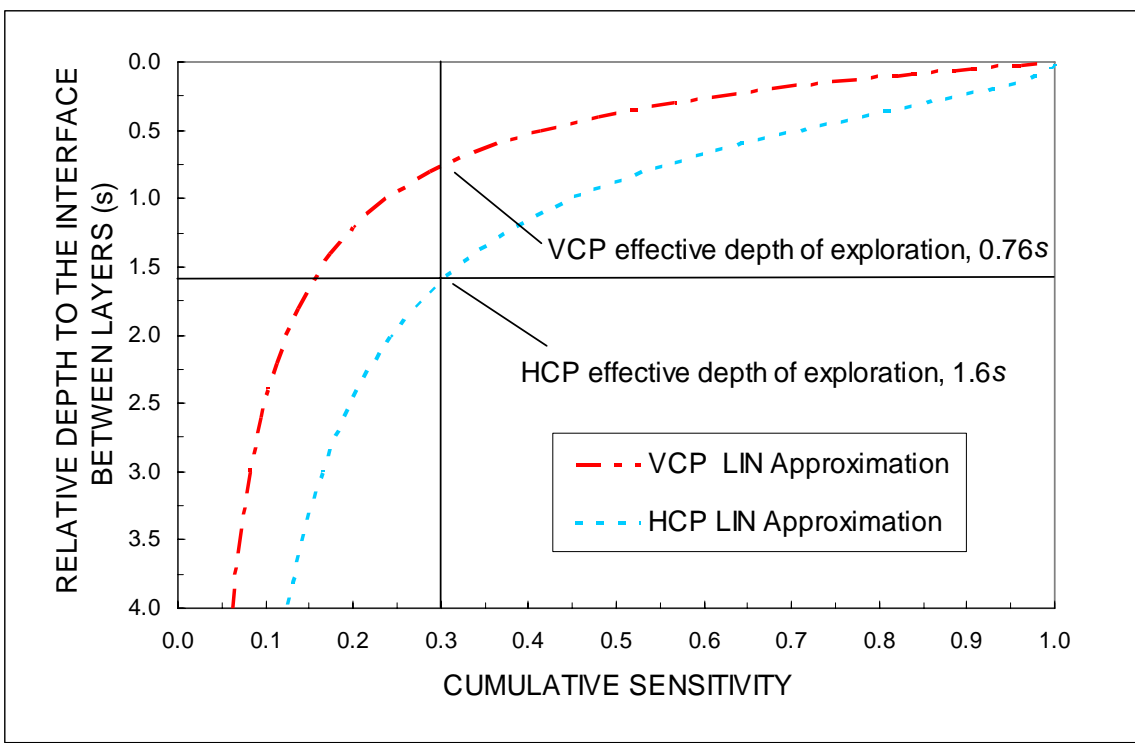
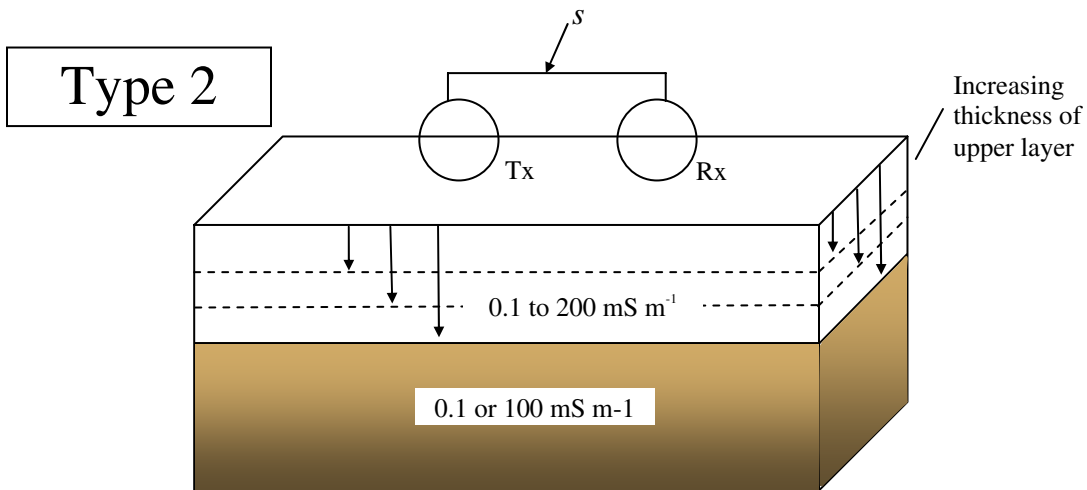
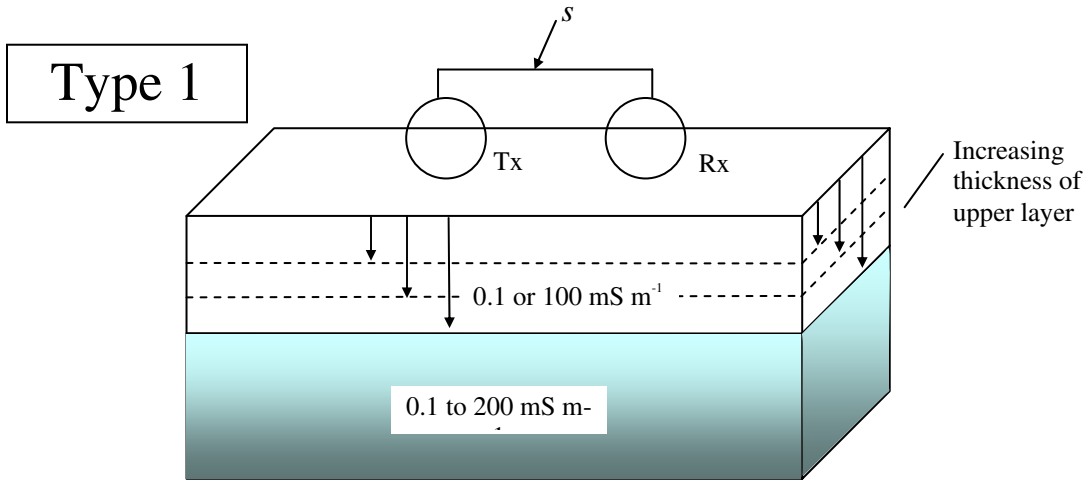


Figure 2. Cumulative sensitivity and relative depth to interface between layers, McNeill (1980). Approximations are for vertical (VCP) and horizontal (HCP) coplanar coil orientations. McNeill's "effective depth of exploration" is indicated by a cumulative sensitivity value of 0.3. Cumulative sensitivity of low-induction-number (LIN) instruments is calculated from infinity to a given relative depth. Relative depth is depth divided by intercoil separation.



3 Figure 3. Each set of cumulative-sensitivity simulations was based on a two-layer soil. Electrical
 4 conductivity of the upper layer in soil model Type 1 and the lower layer in soil model Type 2
 5 were fixed at 0.1 mS m^{-1} for the electrically resistive case or 100 mS m^{-1} for the electrically
 6 conductive case. The variable electrical-conductivity layer was given values ranging from 0.1 to
 7 200 mS m^{-1} . For a given two-layer soil model in each set of simulations, the thickness of the
 8 upper layer increased from 0.001m to 18 m . Tx indicates transmitter coil; Rx indicates receiver
 9 coil; and s is intercoil separation.

10

11

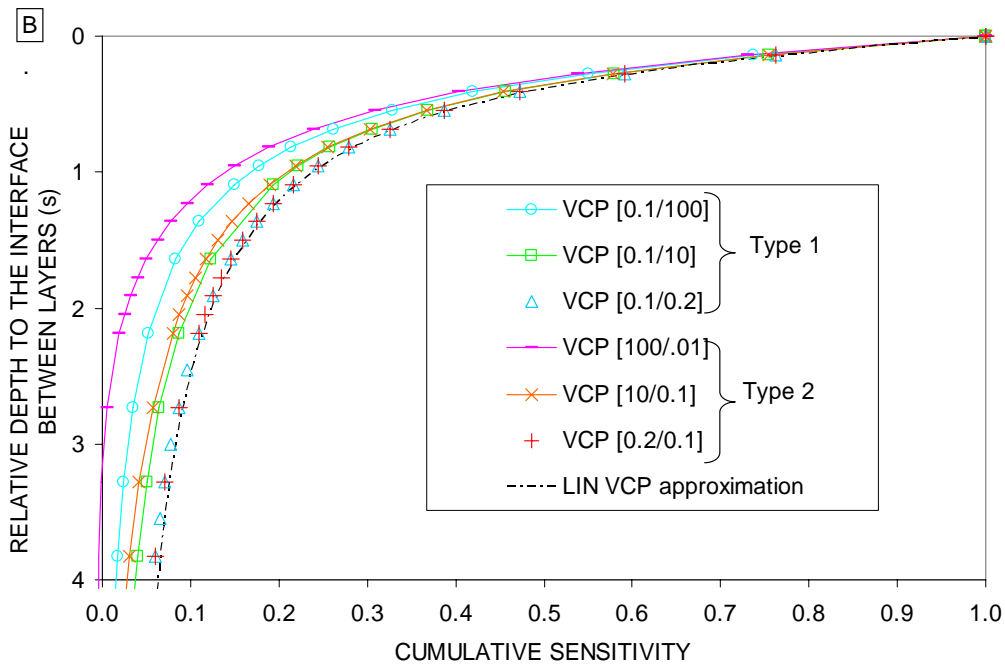
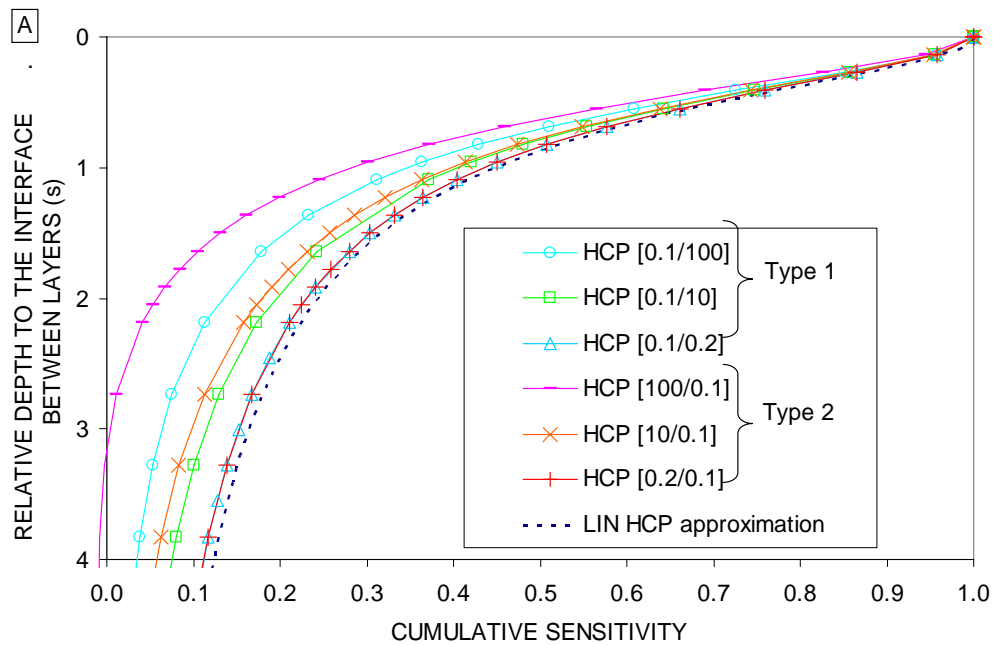


Figure 4. Cumulative sensitivity for soil model Types 1 and 2 calculated from forward numerical simulation results compared with low-induction-number (LIN) approximation. (A) horizontal (HCP) and (B) vertical (VCP) coplanar coil orientation. Relative depth is depth divided by intercoil separation. The first number in brackets is the upper layer electrical conductivity, in mS m^{-1} ; the second number is lower layer electrical conductivity. In (B), to show underlying LIN VCP approximation curves, the lines for the VCP [0.1/0.2] and [0.2/0.1] soil models were removed.

1
2
3
4
5
6
7
8
9
10
11
12
13
14
15
16
17
18
19
20
21
22
23
24
25
26
27
28
29
30
31
32
33
34
35
36
37
38
39
40
41
42
43
44
45
46
47
48
49

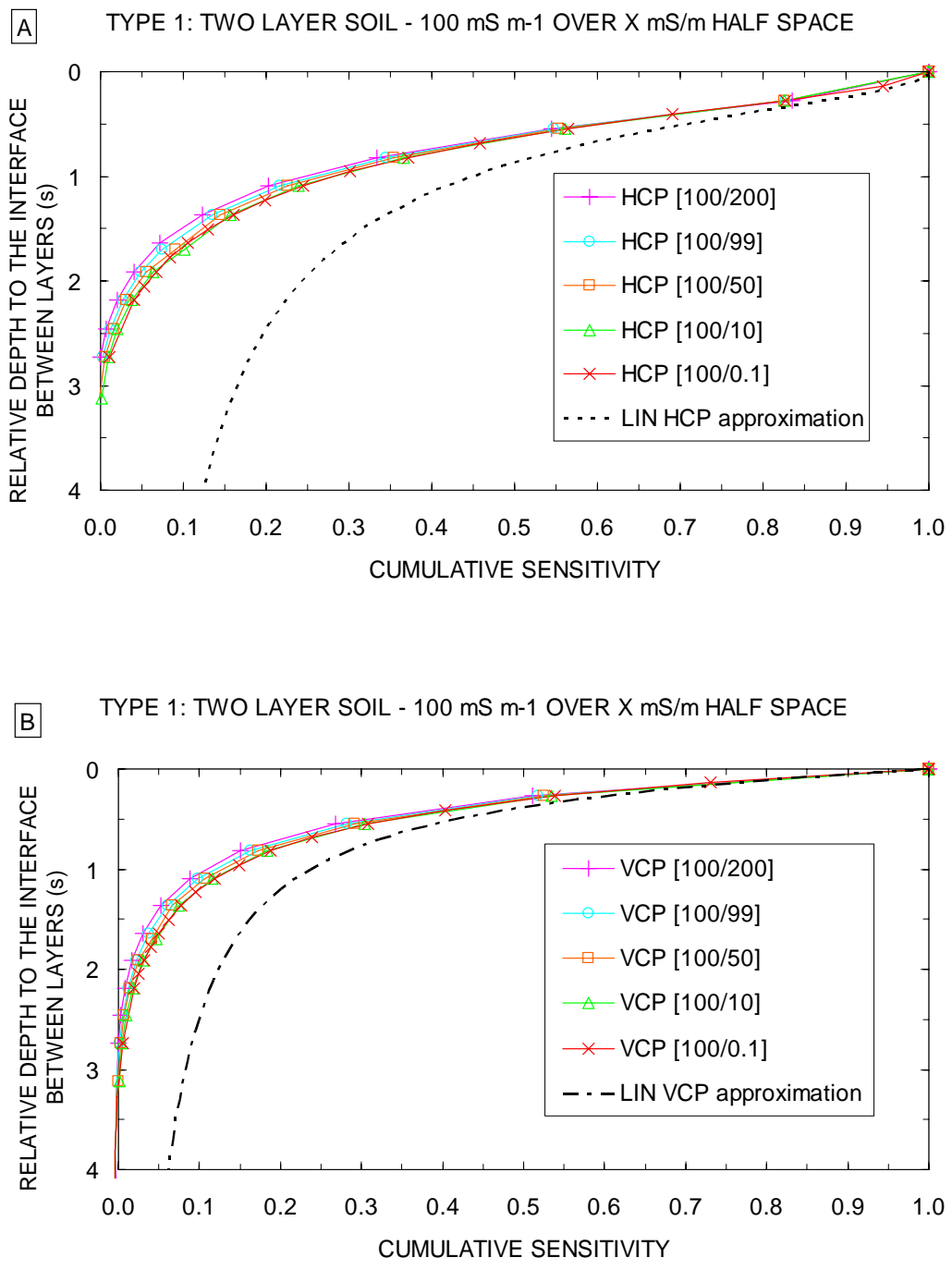
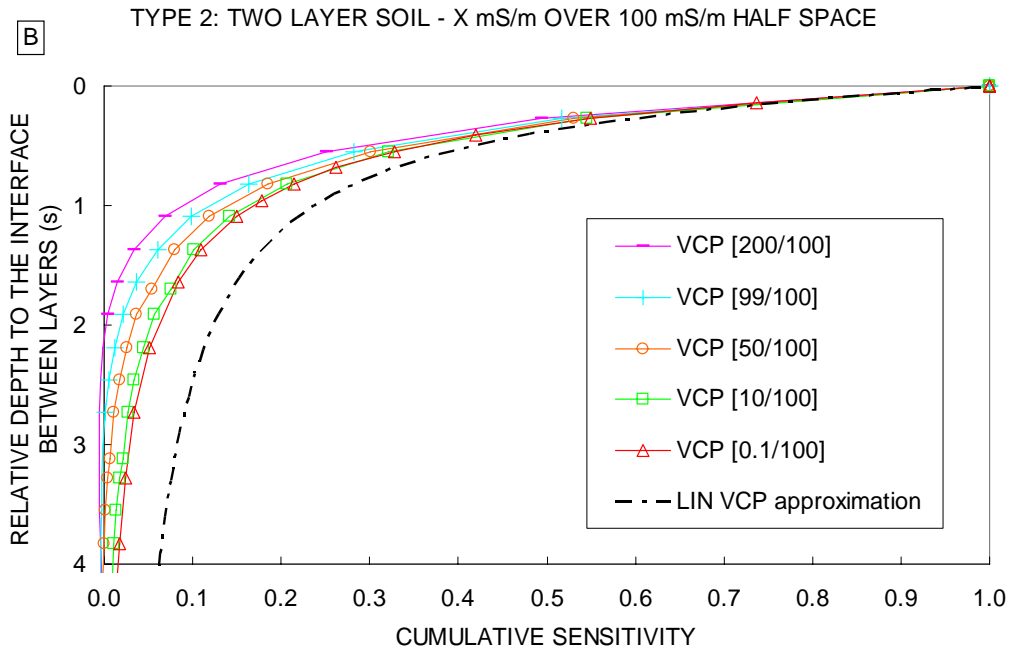
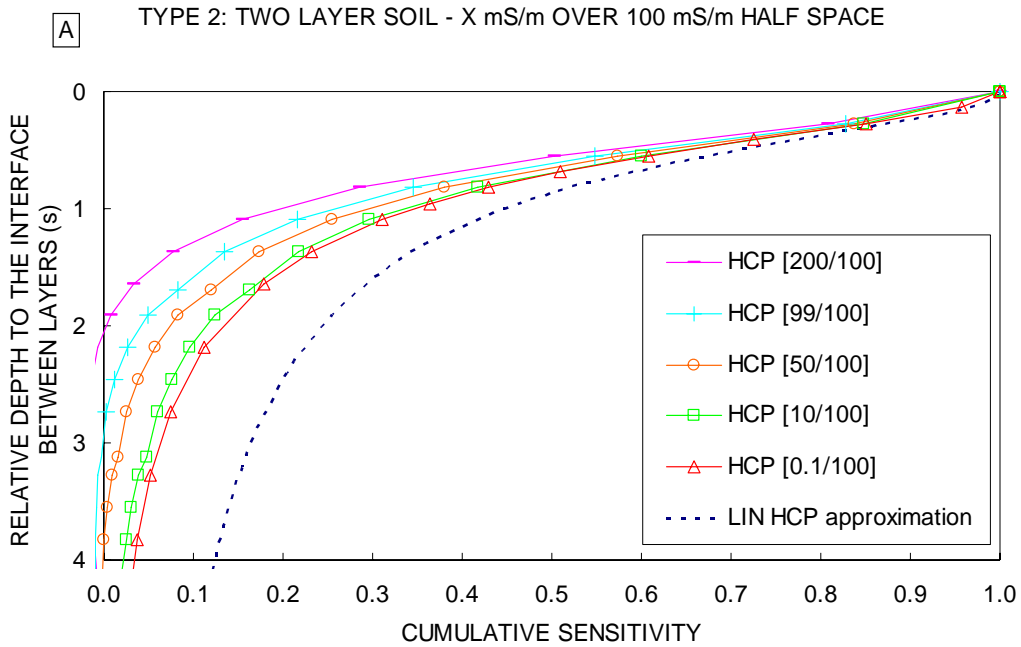
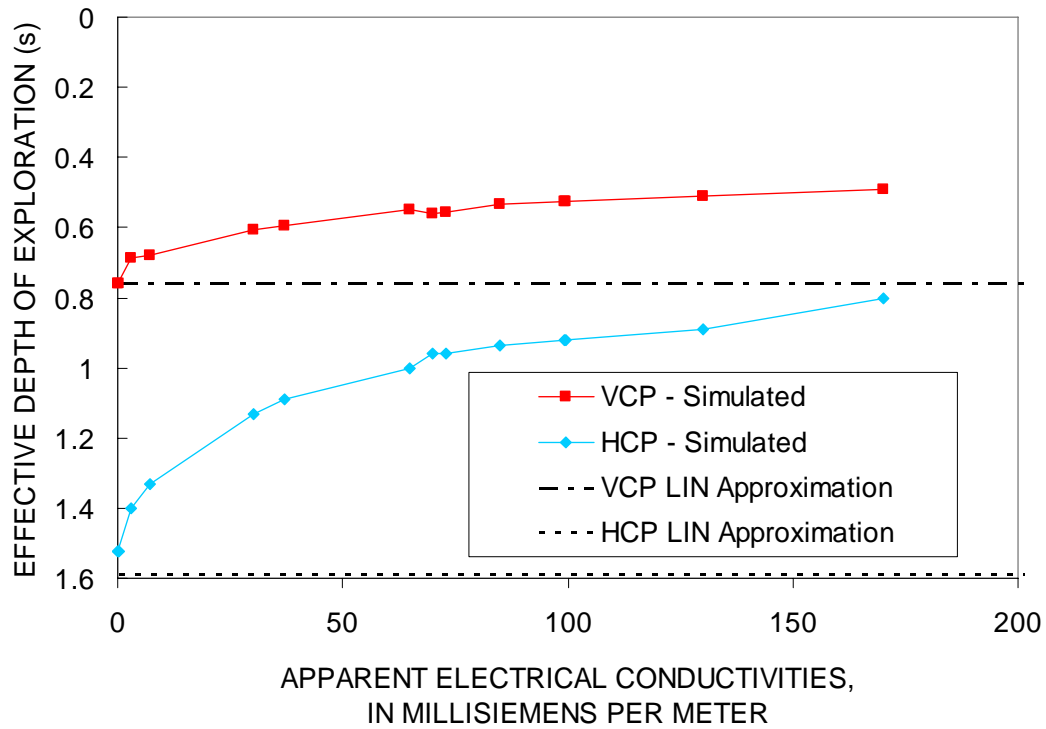


Figure 5. Soil model Type 1 cumulative sensitivity using the higher electrical conductivities sometimes detected in environmental investigations. Comparison of results of forward numerical simulation results with the low-induction-number (LIN) approximation. (A) is horizontal (HCP) and (B) is vertical (VCP) coplanar coil orientation. Relative depth is depth divided by intercoil separation. The first number in brackets is the upper layer electrical conductivity, in mS m⁻¹, the second number is that of the lower layer.



45 Figure 6. Soil model Type 2 cumulative sensitivity using the higher electrical conductivities
46 sometimes detected in environmental investigations. Comparison of results of forward numerical
47 model simulation results with the low-induction-number (LIN) approximation. (A) is horizontal
48 (HCP) and (B) is vertical (VCP) coplanar coil orientation. Relative depth is the depth divided by
49 the intercoil separation. The first number in brackets is the upper layer electrical conductivity, in
50 mS m^{-1} , the second number is the lower layer electrical conductivity.



1
 2 Figure 7. Relation between apparent electrical conductivity and effective depth of exploration:
 3 comparison of simulated and LIN approximation results. VCP, vertical coplanar coil orientation;
 4 HCP, horizontal coplanar coil orientation. Effective depth of exploration is the depth divided by
 5 the intercoil separation.
 6